Exelon.
Generation

NP-11-0024
June 16, 2011

10 CFR 52, Subpart A

U.S. Nuclear Regulatory Commission
ATTN: Document Control Desk
Washington, DC 20555-0001

Subject: Exelon Nuclear Texas Holdings, LLC
Victoria County Station Early Site Permit Application
Response to Request for Additional Information Letter No. 09
NRC Docket No. 52-042

Attached are responses to NRC staff questions included in Request for Additional Information (RAI) Letter No. 09, dated May 6, 2011, related to Early Site Permit Application (ESPA), Part 2, Sections 02.05.01 and 02.05.03. NRC RAI Letter No. 09 contained twenty-three (23) Questions. This submittal comprises a partial response to RAI Letter No. 09, and includes responses to the following six (6) Questions:

02.05.01-2	02.05.03-1
02.05.01-6	
02.05.01-9	
02.05.01-18	
02.05.01-19	

When a change to the ESPA is indicated by a Question response, the change will be incorporated into the next routine revision of the ESPA, planned for no later than March 31, 2012.

Attachment 1A of this letter contains proprietary information. Accordingly, it is requested that Attachment 1A be withheld from public disclosure in accordance with 10 CFR 2.390, "Public inspections, exemptions, requests for withholding." A redacted, non-proprietary version is provided in Attachment 1. An affidavit certifying the basis for this application for withholding as required by 10 CFR 2.390(b)(1) is included as Attachment 1B.

Of the remaining seventeen (17) RAIs associated with RAI Letter No. 09, responses to six (6) Questions were submitted to the NRC in Exelon Letter NP-11-0022, dated June 2, 2011. The response to RAI Question 02.05.01-3, 02.05.01-4, 02.05.01-7, 02.05.01-8, 02.05.01-10, 02.05.01-14, 02.05.01-15, and 02.05.01-16 will be provided by July 5, 2011. The response to RAI Question 02.05.01-20 will be provided by July 20, 2011. The response to RAI Questions

02.05.01-5 and 02.05.01-12 will be provided by August 4, 2011. These response times are consistent with the response times described in NRC RAI Letter No. 09, dated May 6, 2011.

Regulatory commitments established in this submittal are identified in Attachment 7.

If any additional information is needed, please contact David J. Distel at (610) 765-5517.

I declare under penalty of perjury that the foregoing is true and correct. Executed on the 16th day of June, 2011.

Respectfully,

Marilyn C. Kray

Marilyn C. Kray
Vice President, Nuclear Project Development

Attachments:
1. Question 02.05.01-2 (Non-Proprietary Version)
1A. Question 02.05.01-2 (Proprietary Version)
1B. Question 02.05.01-2 Affidavit
2. Question 02.05.01-6
3. Question 02.05.01-9
4. Question 02.05.01-18
5. Question 02.05.01-19
6. Question 02.05.03-1
7. Summary of Regulatory Commitments

cc: USNRC, Director, Office of New Reactors/NRLPO (w/Attachments)
USNRC, Project Manager, VCS, Division of New Reactor Licensing (w/Attachments)
USNRC Region IV, Regional Administrator (w/Attachments)

RAI 02.05.01-2:

Question:

In these questions the growth faults identified in the SSAR are referred to as faults D, E, and K, whether interpreted in subsurface or surficial data sets.

In SSAR Section 2.5.1, several figures illustrate various data sets (seismic reflection, GeoMap, aerial photography, and LiDAR) that lead to your interpretations about the growth faults in the VCNPP vicinity. In order to understand the link between these data and the subsequent interpretations of growth fault structures, and in accordance with 10 CFR 100.23 (d)(2), please provide:

a) A plan-view figure with a scale similar to Figure 2.5.1-41 (i.e., extending a little beyond the 5-mile radius) that contains the following information:

- plant boundary, power block outline, outline of the cooling water basin, and the locations of US Route 77 and McFaddin Rd.
- locations of geotechnical boreholes and cross-section lines from Figures 2.5.1-34 and -35 and 2.5.4-14, -15, -16.
- LiDAR traces for faults D and E and the interpreted zones of deformation bounding these faults.
- LiDAR hillshade base map
- aerial photo lineaments
- GeoMap locations of faults D, E and K as projected to the surface.
- location of the seismic reflection lines and the point locations where faults D, E and K fall on those lines.
- electronic version of this figure that can be magnified to examine the details.

b) A figure that contains a subset of the previous request that includes the LiDAR lineaments from Figure 2.5.1-42, the air photo lineaments from Figure 2.5.1-37 and the GeoMap fault traces from Figure 2.5.1-40 on the LiDAR base map.

Response:

Five figures are provided in the attached response to address the NRC request. The details of these figures are described below.

- Figure 1a – The figure requested as described in part (a) of this RAI question. There is no “zone of deformation” mapped for the lineament associated with growth fault E. Such a zone was not defined as part of the VCS ESP because of the considerable distance between the lineament and the safety related systems, structures, and components that are within the power block area. The points where faults GM-D and GM-K “fall on” the seismic reflection lines are shown for lines GDI, GSI, and TGS. These points are the surface location of the up-dip extent of the faults as identified in the seismic reflection data (see SSAR Figures 2.5.1-45 to 2.5.1-48 and SSAR Table 2.5.1-4). The location of GM-E is not shown on GDI, GSI and TGS because, as stated in SSAR Section 2.5.1.2.4.2.3.1.3, GM-E is not observed in the seismic reflection data. Also note that McFaddin Rd. is labeled as “Farm-to-market Road 445” in the figure consistent with the labels used in the VCS SSAR (see SSAR Figure 2.5.1-39). The seismic reflection profile locations are proprietary data that cannot be publicly released, so this figure is not for public release.

- Figure 1b – This figure is a publicly releasable version of Figure 1a. Figure 1b is the same as Figure 1a, but without the proprietary seismic reflection profile locations presented in Figure 1a.
- Figure 1c – A version of Figure 1a with a smaller extent (i.e., larger scale) so that the details of the cross-section lines and borehole labels can be easily seen. The seismic reflection profile locations are proprietary data that cannot be publicly released, so this figure is not for public release.
- Figure 1d – This figure is a larger-scale version of Figure 1b that allows the details of the cross-section lines and borehole labels to be easily seen. Figure 1d is for public release and does not show the location of proprietary seismic reflection profile locations presented in Figure 1c.
- Figure 2 – The figure requested as described in part (b) of this RAI question.

Associated ESPA Revision:

No ESPA revision is required as a result of this response.

Proprietary Information Deleted

Figure 1a. Map of the VCS Site Area Illustrating Requested Information Including Seismic Reflection Lines (Proprietary).

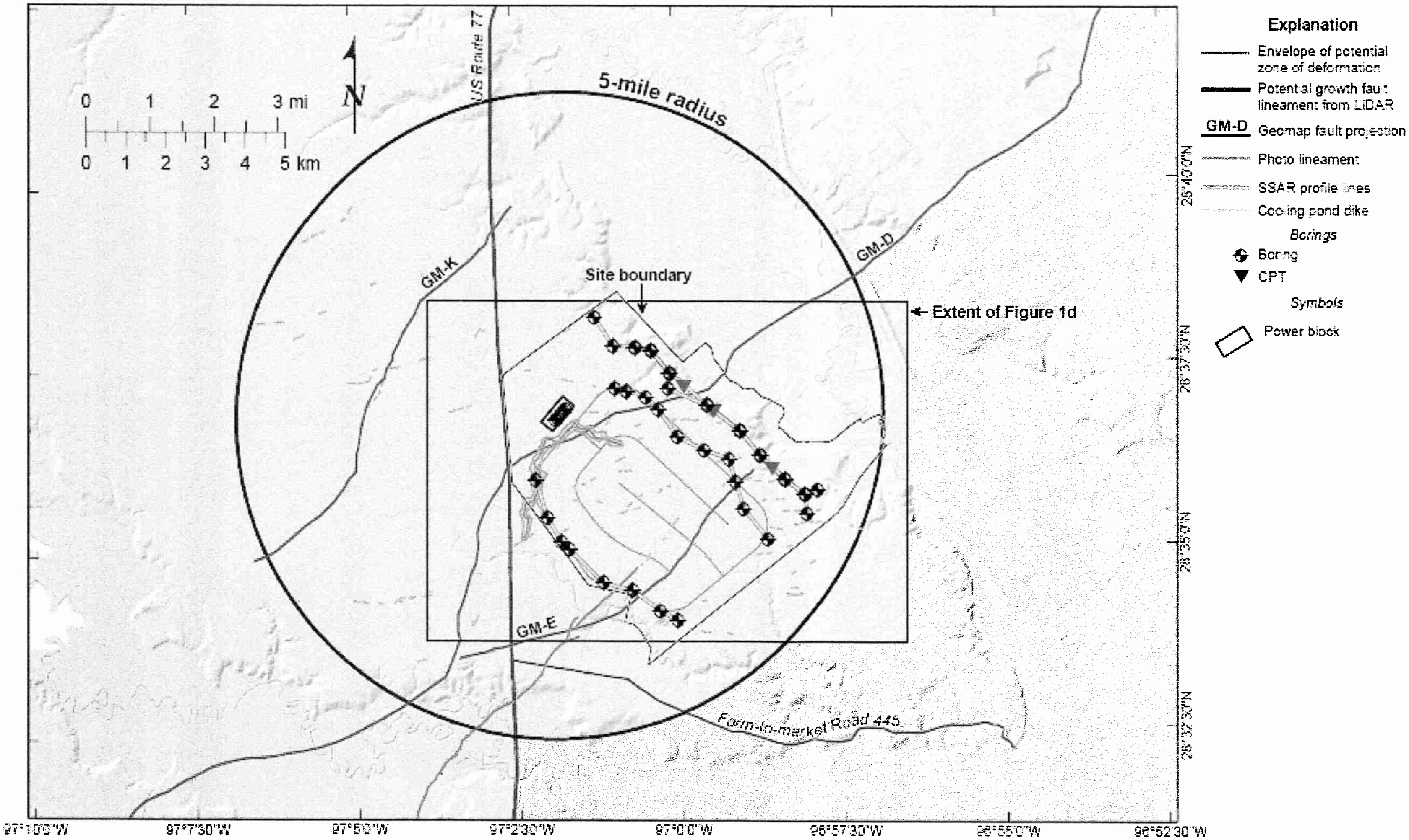

Figure 1b. Map of the VCS Site Area Illustrating Requested Information without Seismic Reflection Lines.

Proprietary Information Deleted

Figure 1c. Detailed Map of the VCS Site Area Illustrating Requested Information with Seismic Reflection Lines (Proprietary).

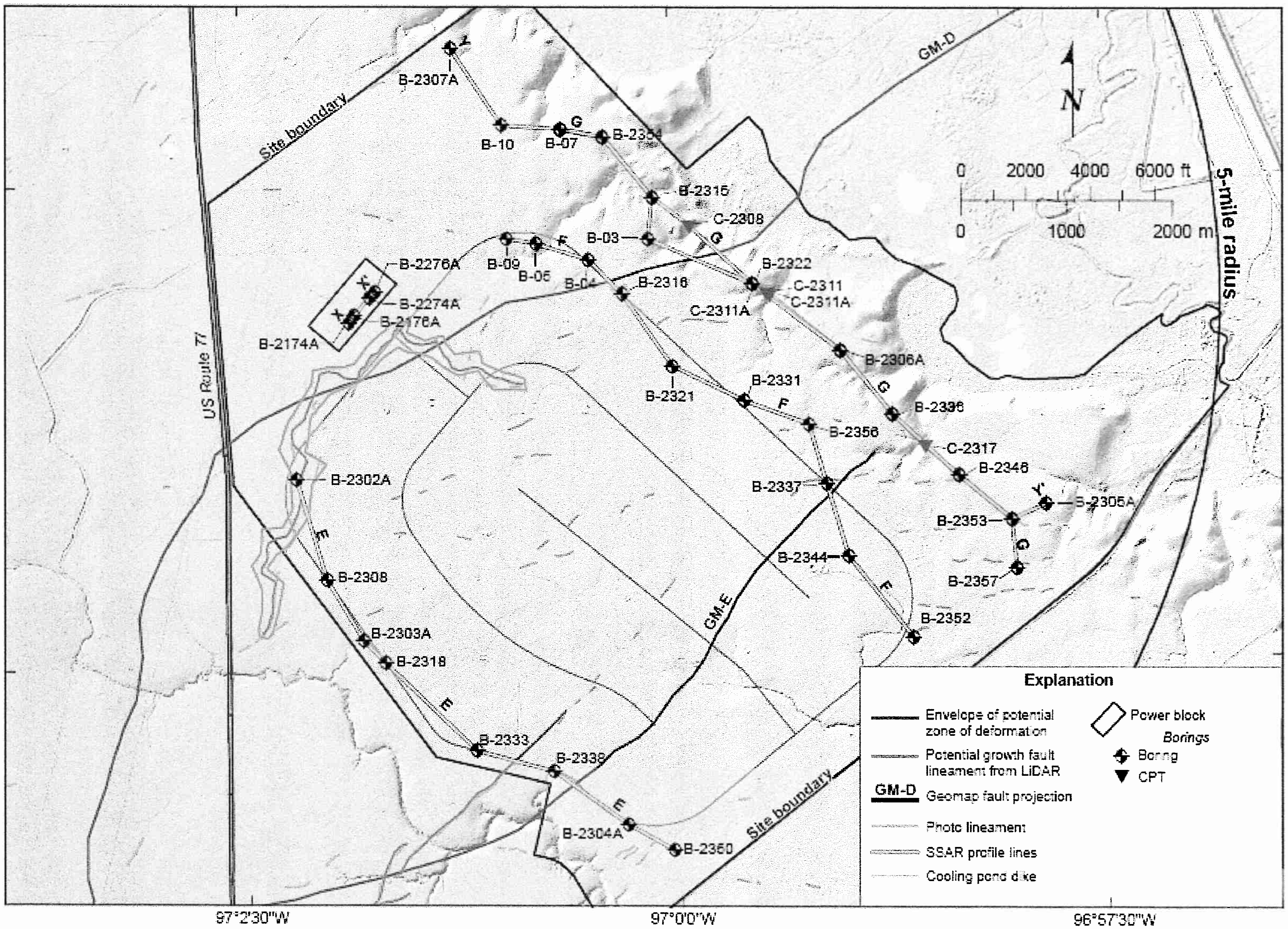

Figure 1d. Detailed Map of the VCS Site Area Illustrating Requested Information without Seismic Reflection Lines.

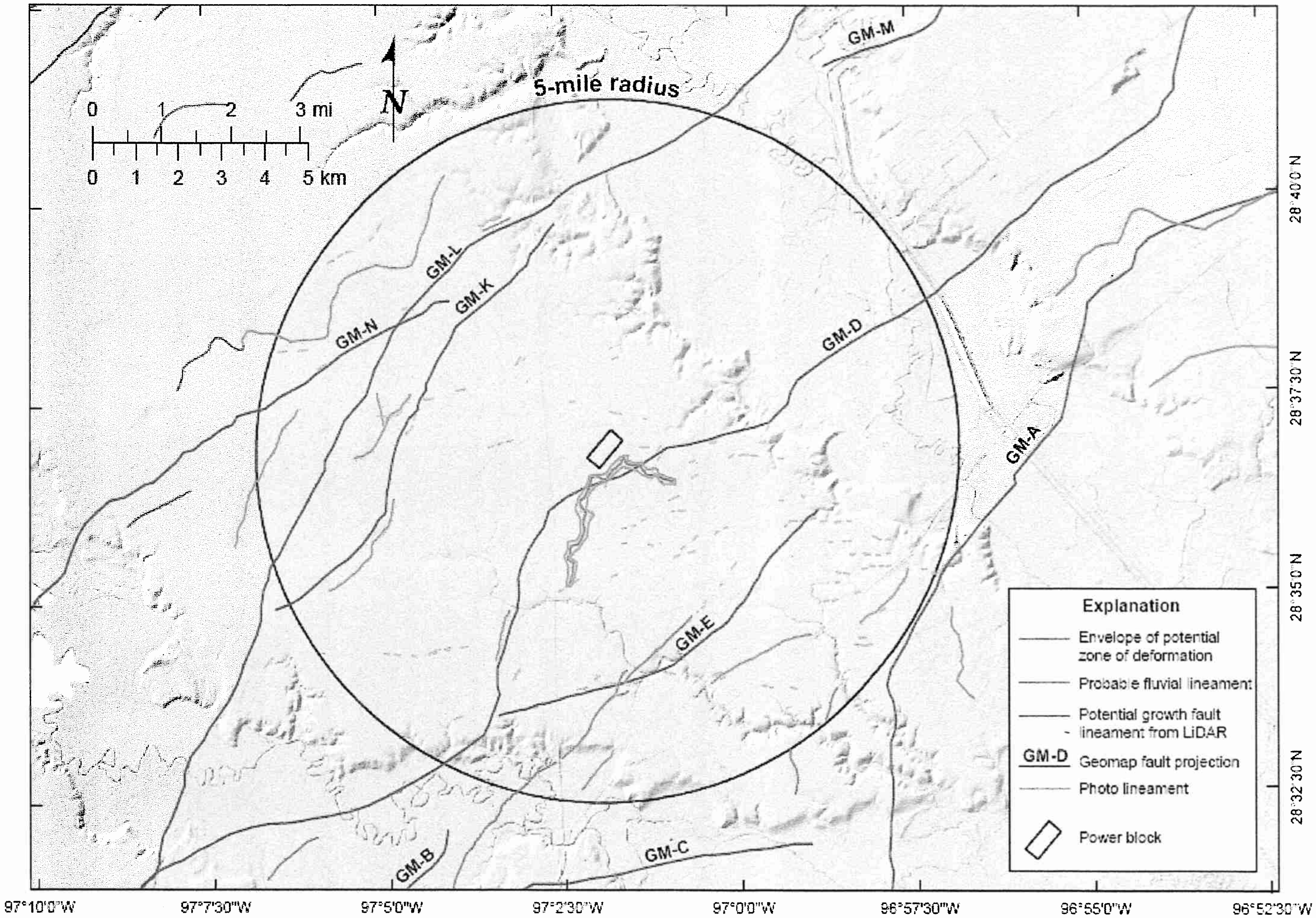

Figure 2. Shaded Relief Map of the VCS Site Area with Requested Lineaments and Geomap Fault Projections.

Question 02.05.01-2 Affidavit

(1 Page)

AFFIDAVIT

I, Julie Kay Hardie, Vice President - Legal, Seismic Exchange, Inc., do hereby affirm and state:

1. I am authorized to execute this affidavit on behalf of Seismic Exchange, Inc. (Seismic Exchange) and have knowledge of the subject matter described herein.
2. Seismic Exchange has provided certain proprietary geophysical data and information (Proprietary Information) to Exelon Generation Company, LLC (Exelon) for use in developing its Early Site Permit Application (ESPA), and response to NRC Request for Additional Information Item No. 02.05.01-2. This Proprietary Information concerns Data and Derivatives of seismic reflection data, which should be held in confidence by the NRC and exempt from public disclosure pursuant to the policy reflected in 10 CFR 2.390(a)(4) & (9) because:
   a. This Proprietary Information: (i) constitutes highly valuable confidential information and trade secrets of Seismic Exchange; (ii) is owned and held in confidence by Seismic Exchange; and (iii) is licensed to Exelon pursuant to that Master Geophysical Data-Use License dated February 29, 2008, which contains strict confidentiality and non-disclosure obligations on the part of Exelon with regard to the Proprietary Information that is the subject matter of this Affidavit and the ESPA.
   b. It is the ordinary course of business and the customary practice and procedure of Seismic Exchange to maintain and require confidentiality and non-disclosure of its proprietary geophysical data, including the Proprietary Information described herein.
   c. Seismic Exchange understands that this Proprietary Information is being transmitted to the NRC voluntarily and in confidence.
   d. This Proprietary Information is neither in the public domain nor available in public sources and could not be gathered readily from other publicly-available information.
   e. Public disclosure of this Proprietary Information would create substantial and irreparable harm to Seismic Exchange, including its competitive position, as this Proprietary Information contains Seismic Exchange's highly valuable trade secrets and proprietary and confidential information. Furthermore, Seismic Exchange incurred significant costs to acquire the Proprietary Information.
3. Accordingly, Seismic Exchange requests that the designated Proprietary Information be withheld from public disclosure pursuant to 10 CFR 2.390(a)(4) & (9) .

Julie Kay Hardie
Julie Kay Hardie

State of Texas)
) SS
County of Harris)

Sworn and prescribed to before me this 8th day of June, 2011.

Christine Marie Russo
Notary Public

My Commission Expires: 4/18/2012

SEAL

CHRISTINE MARIE RUSSO
NOTARY PUBLIC
STATE OF TEXAS
EXPIRES
4-18-2012

RAI 02.05.01-6:

Question:

In SSAR Section 2.5.1.2.4.2.3.1 you use petroleum industry seismic reflection profiles to determine the style and extent of deformation associated with growth fault D, including young, near-surface deformation. You interpret a triangular zone of "distributed down-to-the-southeast tilting or folding of strata" associated with fault D (Fig. 2.5.1-48) based on the pattern of reflectors in the seismic reflection data. In response to Question 02.05.01-01, ML 102510229, 8/16/2010, you stated that there is no evidence that growth faults D or E break the surface or form fault scarps and restated that seismic reflection data indicates that while fault D offsets the Horizon 1 reflector, above this horizon deformation is described as distributed folding.

The staff notes that these seismic reflection data may not be appropriate to image the upper several hundred meters of strata; in most cases the spectral bandwidth is too small and the sensor spacing is too coarse. Based on the acquisition parameters, processing parameters, and the time-migrated stack sections of the four proprietary profiles (supplemental seismic reflection data provided for review), the effective dominant frequency for interpreted horizons H3 and H4 is about 40 Hz, as measured on the migrated time sections. From the depth ranges of selected horizons (Table 2.5.1-3) staff infer average P-wave velocities between about 1895 m/s and 2120 m/s to a two-way travel-time of about 530 milliseconds. Thus, dominant seismic wavelengths at shallow depths in these data average about 45 to 55 m. Assuming that features smaller than about 1/4 wavelength cannot be resolved, only vertical offsets larger than about 12 m (on the H3 or H4 horizons, for example) would be detectable.

In accordance with 10 CFR 100.23 (d)(2), please justify your conclusions with respect to the safety significance of the shallow faults in light of the significant limits of the seismic reflection data. Please explain why other types of subsurface geophysical exploration, that specifically target the shallowest sedimentary layers, were not used for the characterization of the growth fault(s), especially in locations near and beneath the power block.

Response:

SSAR Subsection 2.5.1.2.4.2.4.1 summarizes the conclusions of the VCS ESP with respect to growth faults within the site area. Restating the main content of this subsection, the ESP stated that:

- Only growth faults D and E show any evidence of potential Quaternary activity;
- Other growth faults within the site area have no evidence of deformation since the Early Pliocene or earlier;
- Growth fault E is over 2.6 miles from the site and does not have the potential to affect the site;
- Potential surface deformation associated with growth fault D approaches no closer than approximately 509 feet to the power block envelope;
- Shallow subsurface deformation associated with growth fault D is interpreted to be characterized by distributed monoclinal fault-propagation folding.

The justifications for these statements are summarized below.

Only growth faults D and E show any evidence of potential Quaternary activity

This conclusion is based on several observations:

- Other than growth faults D and E, there is no evidence of surficial deformation associated with any other growth faults within the site area. This observation is supported by observations made during the field reconnaissance and analyses of the LiDAR data and aerial photos (SSAR Figures 2.5.1-4, 2.5.1-37, and 2.5.1-42).
- All of the growth faults identified in the seismic reflection data, except growth fault D, are observed to not offset continuous reflectors that are significantly deeper than the interpreted Quaternary deposits (SSAR Figures 2.5.1-45, 2.5.1-46, 2.5.1-47 and Table 2.5.1-4).

The potential inability of the seismic reflection data to resolve vertical offsets of 12 m or less described in the RAI question does not impact these conclusions.

Other growth faults within the site area have no evidence of deformation since the Early Pliocene or earlier

This conclusion is primarily based on observations made from the seismic reflection data. In particular, the seismic reflection data demonstrate that none of the growth faults imaged by the reflection data, except growth fault D, are observed to offset Horizon 3 (SSAR Figures 2.5.1-45, 2.5.1-46, 2.5.1-47 and Table 2.5.1-4), interpreted to be a latest Miocene to Early Pliocene horizon (SSAR Subsection 2.5.1.2.4.2.3.1.2 and 2.5.1.2.4.2.3.1.4). As stated within SSAR Subsection 2.5.1.2.4.2.3.1.4, it is difficult to identify discrete displacements in reflectors above Horizon 4 due to the nature of the deposits (near-shore, fluvial-deltaic deposits) and the acquisition parameters for the data (optimized for deep petroleum exploration). However, the continuous reflectors that constrain deformation from all of the other identified growth faults are deeper than Horizon 4 and are imaged well enough to document the absence of active deformation above these growth faults.

Growth fault E is over 2.6 miles from the site and does not have the potential to affect the site

This conclusion is primarily based on the interpretation of the surface trace of the growth fault E and the location of growth fault E as identified in the Geomap data. The resolution of the seismic reflection data is not relevant to this conclusion.

Potential surface deformation associated with growth fault D approaches no closer than approximately 509 feet to the power block envelope

This conclusion is primarily based on the distance between the zone of potential deformation mapped for growth fault D (SSAR Figure 2.5.1-43) and the seismic reflection data that establishes a likely causal relationship between growth fault D and the zone of potential deformation. As described in SSAR Subsection 2.5.1.2.4.2.3.1.4, the resolution of the seismic reflection data, combined with the relatively discontinuous fluvial-deltaic deposits, likely impacts the ability to interpret shallow structures (e.g., those above Horizon 4). However, these potential issues do not have an impact on this conclusion. The zone of potential deformation that defines the 509-foot distance is mapped based on the LiDAR data, not the seismic reflection data. Also, as discussed in the response to RAI 02.05.01-1, the listric nature of growth faults makes it unlikely that deformation associated with growth fault D would extend further north than the zone of potential deformation presented within SSAR Figure 2.5.1-48.

Shallow subsurface deformation associated with growth fault D is interpreted to be characterized by distributed monoclinal fault-propagation folding

The justification for this interpretation is described within SSAR Subsection 2.5.1.2.4.2.3.1.4 and 2.5.1.2.4.2.3.2. Restating the relevant content of those subsections, the interpretation is based on: (1) the lack of an apparent discrete fault reflector above Horizon 4, (2) the southeast-down tilting of reflectors in the hanging wall of growth fault D (SSAR Figure 2.5.1-48), and (3) the spatial correlation of the zone of tilted reflectors with the zone of broad monoclinal tilting or folding observed at the surface (SSAR Figure 2.5.1-48 and 2.5.1-43). In addition, this style of monoclinal tilting and folding is characteristic of deformation associated with growth faults observed elsewhere along the coastal plain of Texas. For example, all of the LiDAR lineaments potentially associated with growth faults within the site vicinity (SSAR Figure 2.5.1-44), as well as growth faults identified in other parts of the Texas coastal plain (FSAR Subsection 2.5S.1.2.4.2.2.2 and FSAR Figure 2.5S.1-46 of STP, 2007), have a similar expression of broad monoclinal tilting and folding.

As described earlier in this response, it is difficult to identify discrete displacements across reflectors above Horizon 4 due to the nature of the deposits and the acquisition parameters for the data. This difficulty is one of the reasons why the "monoclinal fault-propagation folding" is described within the SSAR as an interpretation and not a definite conclusion. It is possible that discrete faulting extends further updip than interpreted in SSAR Figure 2.5.1-48. However, as described in the SSAR and in the response to RAI 02.05.01-1, there is no evidence to support the interpretation that the discrete faulting associated with growth fault D extends to the surface.

The potential uncertainty regarding the style of shallow deformation associated with growth fault D (i.e., at what depth does discrete faulting transition to distributed folding and tilting) is not significant to evaluating the structures, systems, and components (SSCs) important to safety for the VCS site. All of the SSCs that are important to safety are located within the power block envelope presented in SSAR Figure 2.5.1-43. As described above and in the response to RAI 02.05.01-1, the listric nature of growth faults makes it unlikely that potential deformation associated with growth fault D would approach closer to the power block than the 509 feet (155 m) presented in SSAR Figure 2.5.1-43 regardless of whether deformation in the shallow subsurface is dominated by discrete faulting or monoclinal fault-propagation folding. Therefore, the conclusion/interpretation that is the subject of the preceding three paragraphs is not relevant "to the safety significance of the shallow faults."

Other investigative methods, including subsurface geophysical exploration, were not conducted as part of the VCS ESP because the efforts presented within the ESP application are able to demonstrate that: (1) no growth faults project to the surface within the power block area; and (2) the closest approach of potential deformation to the power block area, associated with a growth fault, is no closer than approximately 509 feet. Particular attention was paid to the power block area because the power block area delineates the area within which all safety-related SSCs will be located.

Response References:

STP, *South Texas Project COL application for STP Site, Units 3 & 4, Rev. 5*, NRC Docket Nos. 52-012 and 52-013, accession number ML110340881, 2007.

Associated ESPA Revision:

No ESPA revision is required as a result of this response.

RAI 02.05.01-9:

<u>Question:</u>

In SSAR Section 2.5.1.2.4.2.3 you describe the identification of growth faults from aerial photographs and LiDAR topography shaded-relief maps. The staff observes that both air-photo and LiDAR data (Fig. 2.5.1-37, -38, -42) suggest that growth fault D (or a splay thereof) may extend 1-2 km northeastward instead of turning sharply to the southeast near the power block (**see attached Figure 1**). This may be a more linear trace for Growth fault D that would correspond to the more typical trend of other GeoMap faults in the vicinity. In addition, cross-sections in Figure 2.5.4-15, between boreholes B-04 and B-2316 and Figure 2.5.4-16, between boreholes B-2354 and B-2322, show small (~1 m) steps in topography and 1-3 m apparent offsets of several subsurface units that may be evidence of a fault trending in this direction.

In accordance with 10 CFR 100.23 (d), explain why this potential trend was not considered part of fault D. Please provide an evaluation of the borehole data, cited above, with regard to a possible shallow fault trending northeast rather than southeast. Please discuss the safety implications of this possible fault splay, which would be closer to the power block.

<u>Response:</u>

The above RAI request has multiple parts, which are addressed in the following sections. Section 1 evaluates the alternative lineament locations discussed in the RAI. Section 2 discusses the boring data presented in SSAR Figures 2.5.4-15 and 2.5.4-16 (Profiles F and G) and their potential to constrain the location of growth fault deformation. Section 3 summarizes the safety implications of the alternative lineaments evaluated in response Section 1.

1. Alternative Lineaments Potentially Associated with Growth Fault D

This RAI question included a figure (titled "*USGS RAI 2.5.1-Figure 1*" and referred to here as NRC Figure 1) that shows NRC-proposed alternative traces of the lineament associated with growth fault D. These alternative traces are shown in NRC Figure 1 as two dashed lines trending west from the edge of the Guadalupe River flood plain and merging into one line at approximately the VCS site 0.6-mile radius. The RAI question did not provide the coordinates of the alternative lineaments, so an interpretation of the NRC-proposed alternative lineaments in NRC Figure 1 is presented in Figures 1 and 2 of this RAI response. For ease of discussion, the three components of the NRC-interpreted lineaments are referred to as NRC lineaments A, B, and C (Figure 1). Assumptions have been made in this RAI response regarding the geomorphology along the NRC proposed lineaments and the criteria used by the NRC to map these lineaments. Based on these assumptions, the RAI response systematically evaluates the data available for inferring the NRC proposed lineaments.

Based on the location of the NRC-proposed lineaments as presented in Figure 1, the geomorphology along these proposed lineaments can be described as follows.

NRC lineament A is the westernmost of the NRC-identified lineaments (labeled "Prominent LiDAR lineament" on NRC Figure 1) and is mapped along the base of an approximately east-west-trending topographic break.

NRC lineament B appears in NRC Figure 1 as an eastward extension of NRC lineament A (labeled "LiDAR lineament (modified by pond construction?)" in NRC Figure 1). NRC lineament B bisects two northwest-trending low-relief ridges and a circular depression (Figure 1). At its easternmost extent, NRC lineament B is coincident with a west-southwest-trending erosional gulley (Figure 2).

NRC lineament C appears in NRC Figure 1 as an east-northeast extension of NRC lineament A (labeled "Alternative trace or splay of fault D" in NRC Figure 1). The majority of NRC lineament C is mapped in the center of a northeast-striking erosional gulley and the easternmost extension of the splay is coincident with a low-relief south-facing topographic break on the Guadalupe River flood plain (Figures 1 and 2).

As described in SSAR Subsection 2.5.1.2.4.2.2, lineaments interpreted in LiDAR-derived topography were analyzed as part of the VCS ESP application and classified as either potentially related to growth faults or probably related to fluvial process (see SSAR Figure 2.5.1-44). The criteria used to make these determinations (described in detail in SSAR Subsection 2.5.1.2.4.2.2) included:

- The degree of linearity and consistency of expression;
- The degree of lateral continuity;
- The presence of cross-cutting relationships; and
- The presence of deflected or otherwise modified fluvial systems.

Using these criteria, and the geologic maps developed as part of the VCS ESP project site (SSAR Figure 2.5.1-5), the NRC-proposed lineaments can be evaluated to determine whether they are potentially related to growth faults or probably related to fluvial process. NRC lineament A is mapped along the base of a 1,600-ft-long (500-m-long) south-facing east-west-trending topographic break. This topographic break was identified on aerial photography (SSAR Figure 2.5.1-37). However, upon more detailed inspection of the LiDAR data during construction of the site geologic map, it was determined that this topographic break is the margin of a subunit within the Beaumont Formation (Unit Qbc). As discussed in SSAR Subsection 2.5.1.2.4, Unit Qbc consists of levee and flood plain deposits that form locally raised topography consisting of silt, clay and minor amounts of sand and gravel. This particular Qbc deposit forms a northwest-striking lobe (i.e., raised deposit) with generally parallel boundaries (Figure 1 and SSAR Figure 2.5.1-5). As shown in Figure 1, the northern north-facing margin of the Qbc lobe is parallel to NRC lineament A, and, at the east end of NRC lineament A, both margins of the Qbc lobe make parallel turns south-southeast across NRC lineaments B and C. These parallel margins of the lobe support the conclusion that the raised deposit is not related to surface deformation from growth faulting. In addition, there are no topographic breaks or steps crossing the Qbc lobe coincident with any of the NRC-proposed lineaments (Figure 1) further supporting the conclusion that the NRC-proposed lineaments do not have any post-Beaumont deformation observable within the Qbc lobe. Therefore, it does not appear that NRC proposed lineament A is related to surface deformation associated with growth fault D.

Similarly, the available geomorphic observations along NRC-proposed lineaments B and C do not support the interpretation that these lineaments represent a possible northeast extension of growth fault D (Figures 1 and 2). These NRC-proposed lineaments do not meet the criteria used as part of the VCS ESP to identify potential growth fault lineaments (see SSAR Subsection 2.5.1.2.4.2.2). For example:

- The NRC-proposed lineaments do not have a distinct and consistent linear expression;
- The degree of lateral continuity of the proposed lineaments is low or non-existent where they are not associated with erosional gullies;
- The proposed lineaments are coincident with parallel topographic lineaments likely related to fluvial depositional process where the proposed lineaments are mapped across older landforms (e.g., Qbc lobes) (see discussion above regarding NRC lineament A); and
- The proposed lineaments do not appear to deflect, modify, or influence any drainages along their map trace.

As evidence of this last point, NRC lineament B crosses two generally northwest-trending low-relief topographic ridges, and there is no apparent offset, topographic step, or monoclinal folding in the ridges that appear related to the proposed lineament (Figure 1). For example, two northeast-trending photo lineaments are mapped across the western of the two northwest-trending ridges, but these lineaments are not mapped coincident with a step in topography consistent with other growth fault lineaments and these lineaments are mapped over only short distances (i.e. no lateral continuity). Similarly, NRC lineament C is mapped largely within a northeast-trending erosional gully, not along the margin of a southeast-facing topographic lineament that appears related to growth faulting. Therefore, the NRC-proposed lineaments were not considered to be associated with growth fault D.

2. Borehole data from Profiles F and G

In the this RAI question, the NRC describes their observation of "small (~1 m) steps in topography between boreholes" and "1-3 m apparent offsets of several subsurface units" along the cross sections presented in SSAR Figures 2.5.4-15 and 2.5.4-16 (profiles F and G, respectively) as potential evidence of deformation related to growth faulting. The surface topography included within these profiles is based on drawing a straight line between the elevations of the widely spaced borings. Given the coarse sampling along these profiles (on the order of one elevation value every 1000 feet), they cannot be used to evaluate the presence or absence of surface deformation potentially related to growth faulting. In addition, Figure 2 shows that the variations in topography observed within these profiles are likely due to the erosional and fluvial geomorphology along the elevated margin of the Guadalupe River floodplain, not growth faulting (Figure 2).

The borehole spacing, combined with the depositional characteristics of the Beaumont Formation, also make the interpretation of small elevation changes (1-3 m) between subsurface units difficult to evaluate. As stated in SSAR Subsection 2.5.1.2.3, the Beaumont Formation is very heterogeneous and composed of multiple noncontinuous soil types deposited within transgressive, aggradational, and progradational environments (Blum and Aslan, 2006; Winker, 1979). Thus, the elevation change between stratigraphic units and lateral heterogeneity of the stratigraphy is more likely a result of normal fluvial-deltaic depositional and erosional processes that create deposits of variable thickness, rather than faulting. Given the chaotic nature of Beaumont Formation subunits and the borehole spacing across growth fault D, the borehole data presented in SSAR Figures 2.5.4-15 and 2.5.4-16 cannot be used to evaluate the presence or absence of deformation related to growth faults.

3. Safety Implications

The proposed NRC lineaments do not have safety implications to the VCS Site because:

- The proposed lineaments do not appear to be lineaments potentially related to growth faults (see discussion in section 1); and

- The proposed lineaments do not approach any closer to the power block than the zone of deformation associated with growth fault D (see Figure 1 which shows a 509 ft, 155 m, buffer around the power block and SSAR Figure 2.5.1-43), and the power block will contain all safety related systems, structures, and components.

Response References:

Blum, M. D. and Aslan, A., *Signatures of climate vs. sea-level change within incised valley-fill successions: Quaternary examples from the Texas Gulf Coast*: Sedimentary Geology, v. 190, p. 177-211, 2006.

Winker, C. D., *Late Pleistocene Fluvial-Deltaic Deposition: Texas Coastal Plain and Shelf* [MA thesis]: Austin, TX, University of Texas at Austin, 1979.

<u>Associated ESPA Revision:</u>

No ESPA revision is required as a result of this response.

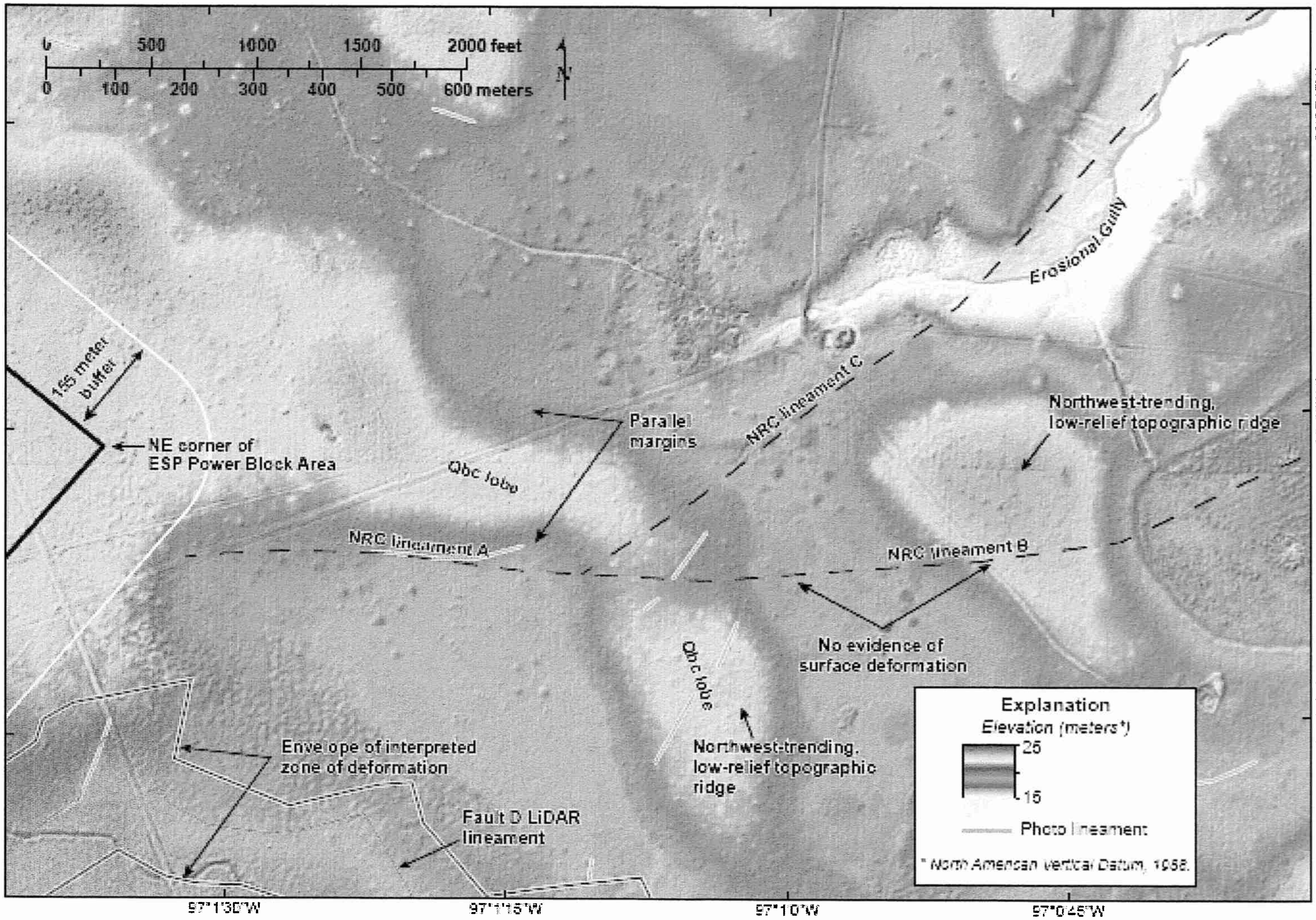

Figure 1. Color Shaded Relief Map with the NRC LiDAR Lineaments.

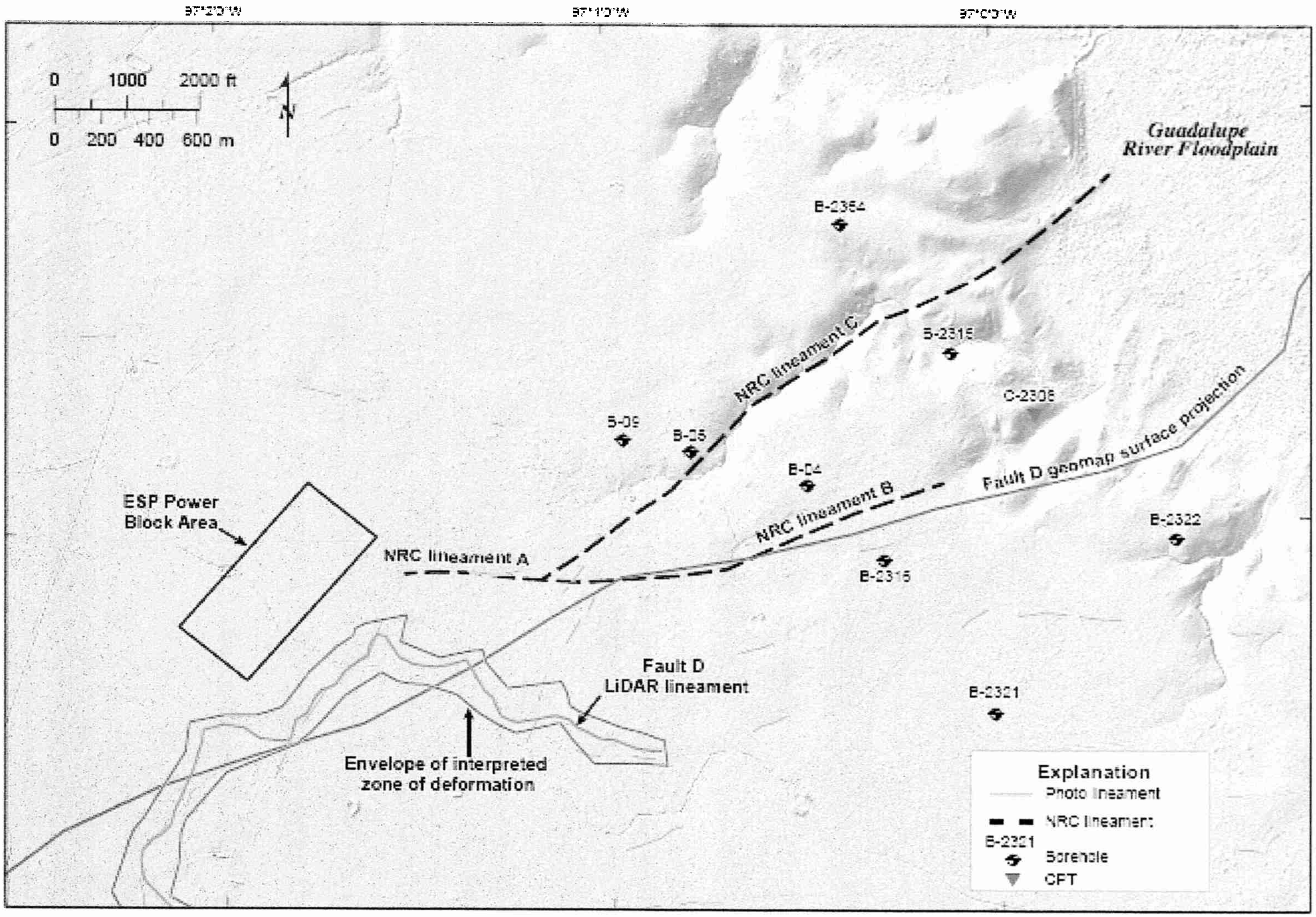

Figure 2. Shaded Relief Map of the NRC LiDAR Lineaments and Selected Geologic Borings.

RAI 02.05.01-18:

Question:

In SSAR section 2.5.1.2.4.2 you stated that the Vicksburg growth faults most proximal to the site overlay the San Marcos Arch, a region with relatively little salt, so many of the growth faults in this area are associated with shale ridges, massifs, or diapirs. In support of 10 CFR 100.23 (d), please discuss the evidence for these shale features associated with the Vicksburg faults in the VCS vicinity and illustrate the location of any shale ridges, massifs or diapirs present in the VCS vicinity.

Response:

As summarized in SSAR Section 2.5.1.2.4.2, many of the Vicksburg growth faults most proximal to the VCS site are associated with shale features such as shale ridges, massifs, or diapirs. The association between the Vicksburg growth faults and shale features has been established through industry-standard investigation practices (e.g., analysis of seismic reflection lines and borehole data) and has been reported in numerous peer-reviewed scientific articles (e.g., Bruce, 1973; Combes, 1993; Culotta, et al., 1992; Diegel, et al., 1995; Erxleben and Carnahan, 1983). In general, these studies report that Vicksburg growth faults sole into either: (1) the upper sections of the Jackson or Vicksburg shales, or (2) within the deeper Clairborne and Midway Group shales of the Paleocene and Eocene section (Bruce, 1973; Combes, 1993; Culotta, et al., 1992; Diegel, et al., 1995; Erxleben and Carnahan, 1983). For example, Culotta et al. (1992) interpret a 155-mi-long (250-km-long) seismic survey across the San Marcos Arch parallel to the western edge of Jackson County (the county to the east of Victoria County) and identify Vicksburg growth faults soling into a shale diapir within the Jackson and Clairborne Formations at the southern most portion of the seismic line. Similarly, Combes (1993) presents seismic lines in Goliad and Refugio counties (to the west of Victoria County) imaging Vicksburg growth faults that sole into shale features.

The only publicly available regional compilation of shale features within the VCS site vicinity identified during the ESP project is shown in Figure 1. This figure shows the location of 18 shale features that are between approximately 12 and 58 mi (19 to 93 km) from the VCS site (Bishop, 1977; Brooner, 1967). Of these 18 diapirs and ridges, only three diapirs (Dacosta, Una West, and Tatton) and one ridge (Sherriff) are mapped within the VCS site vicinity. These shale features are all cored by Jackson-Vicksburg shale and are mapped within the lower to middle Frio Formation (Bishop, 1977). In general, these shale features are on the order of one square mile (2.4 to 2.8 square kilometers) or less in area (Brooner, 1967).

It should be noted that the locations of shale features within the VCS site vicinity are not widely published. The absence of publicly available data is likely due to the following factors. First, these features commonly are targets of commercial petroleum extraction. Although exploration companies may map their location, these companies in general do not publicly release this information. Second, there is little scientific interest in the location of shale features outside of the petroleum industry, so there are very few independent academic studies of shale features within the VCS site vicinity.

Response References:

Bishop, R. S., *Shale diapir emplacement in south Texas; Laward and Sherriff examples*: Gulf Coast Association of Geological Societies Transactions, v. 27, p. 20-31, 1977.

Brooner, F., *Shale Diapirs of the Lower Texas Gulf Coast as Typified by the North LaWard Diapir*: Gulf Coast Association of Geological Societies, v. 17, p. 126-134, 1967.

Bruce, C. H., *Pressured shale and related sediment deformation: Mechanisms for development of regional contemporaneous faults*: AAPG Bulletin, v. 57, p. 878-886, 1973.

Combes, J. M., *The Vicksburg Formation of Texas: depositional systems distribution, sequence stratigraphy, and petroleum geology*: AAPG Bulletin, v. 77, p. 1942-1970, 1993.

Culotta, R., Latham, T., Sydow, M., Oliver, J., Brown, L. and Kaufman, S., *Deep structure of the Texas Gulf passive margin and its Ouachita Precambrian basement: results of the COCORP San Marcos Arch survey*: AAPG Bulletin, v. 76, p. 270-283, 1992.

Diegel, F., Karlo, J., Schuster, D., Shoup, R. and Tauvers, P., *Cenozoic structural evolution and tectono-stratigraphic framework of the northern Gulf Coast continental margin*, in Jackson, M. P. A., Roberts, D. and Snelson, S., eds., Salt Tectonics: A Global Perspective, AAPG Memoir 65, p. 109-151, 1995.

Erxleben, A. W. and Carnahan, G., *Slick Ranch Area, Starr County Texas*, in Bally, A. W., ed., Seismic Expression of Structural Styles, Volume 2: Tulsa, OK, American Association of Petroleum Geologists, p. 2.3.1-22 to -26, 1983.

Associated ESPA Revision:

No ESPA revision is required as a result of this response.

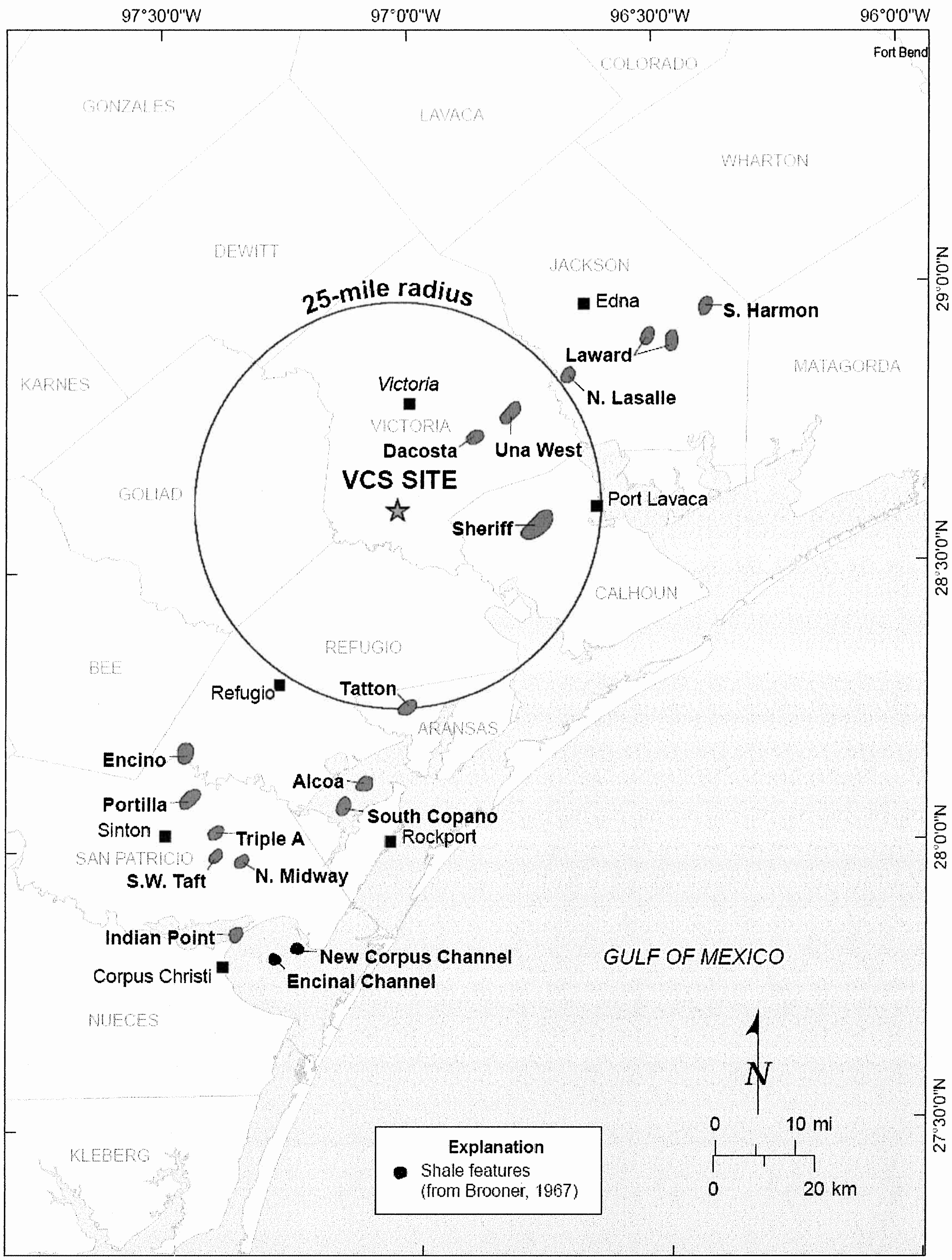

Figure 1. Map of Shale Diapirs and Ridges within the VCS Site Vicinity.

RAI 02.05.01-19:

Question:

In SSAR Section 2.5.1.1, you described the ancestral Mississippi River contributing classic sediments to the Gulf of Mexico beginning in the Late Jurassic to Early Cretaceous (~ 99-191 Ma) and that there was a large change in deposition during the Upper Cretaceous that lead to a widespread unconformity attributed to a major eustatic lowering of sea level. The staff notes that recent publications argue that the Gulf Coast and Mississippi Embayment unconformity can be attributed to the passing of the Bermuda hotspot under the region in Mid-Cretaceous time and that the Mississippi River did not exist until late Cretaceous (Cox & Van Arsdale, 1997; 2002). In support of 10 CFR 100 23 (d) please include this alternative interpretation in the SSAR discussion about the stratigraphy and tectonics of the Gulf of Mexico.

Cox & Van Arsdale, 1997, Hotspot origin of the Mississippi embayment and its possible impact on contemporary seismicity, Engineering Geology, v. 46, n. 3/4, p. 5-12;

Cox & Van Arsdale, 2002, The Mississippi Embayment, North America: a first order continental structure generated by the Cretaceous superplume mantle event. Journal of Geodynamics, v. 34, p. 163-176

Response:

Cox & Van Arsdale (1997) postulate an alternative hypothesis to that proposed by previous investigators for the development of the Mississippi Embayment. Whereas some investigators have related the Late Cretaceous to early Tertiary subsidence of the Mississippi Embayment to the opening of the Gulf of Mexico, more recent data described in Subsection 2.5.1.1.4.3 indicate that the Gulf began to open during the early Jurassic. In summary, Cox & Van Arsdale (1997) contend that the formation of the Mississippi Embayment was coeval with the passage of the Mississippi Valley graben system over the Bermuda hotspot at about 90 Ma; based upon the interpretation of several aspects of geologic data:

- Basal deposits of Upper Cretaceous gravel, flanking the Pascola Arch in the northern embayment, are interpreted as indicating reactivation of the arch.
- Subcrops of Jurassic and Early Cretaceous strata define a southwest-plunging arch in the southern embayment.
- Paleocene sediments nonconformably overlie deeply weathered mid-Cretaceous alkalic plutons along the western margin of the embayment.
- Stratigraphic data suggest that Mississippi River sediments began to enter the Gulf of Mexico during the Late Cretaceous.

Cox & Van Arsdale (2002) provide recently published age dates to further support pre-subsidence uplift of the Mississippi Embayment due to hotspot flux during the Cretaceous superplume mantle event. This alternative hypothesis proposes that the Mississippi River system developed during late Cretaceous subsidence of the Mississippi Embayment and that the Embayment subsided about 60 million years after cessation of sea floor spreading in the Gulf of Mexico. While either alternative hypothesis may be used to explain the tectonic evolution of the Mississippi Embayment and the Gulf of Mexico, neither affects the development of the site-specific probabilistic seismic hazard analysis, ground motion response spectra and site response. A description of the alternate interpretation will be added to a future revision to the ESPA, as described below.

References:

Cox, R.T. and Van Arsdale, R.B., *Hotspot origin of the Mississippi embayment and its possible impact on contemporary seismicity*, Engineering Geology, vol. 46, pp. 201-216, 1997.

Cox, R.T., and Van Arsdale, R.B. *The Mississippi Embayment, North America: a first order continental structure generated by the Cretaceous superplume mantle event*, Journal of Geodynamics, vol. 34, pp. 163-176, 2002.

Associated ESPA Revision:

SSAR subsection 2.5.1.1.3.3.2 will be revised in a future revision to the ESPA as indicated:

In the Gulf of Mexico basin the Upper Jurassic is predominantly marine, with non-marine fluvial and deltaic clastic sediments present in the northern and northwestern basin margins (References 2.5.1-23 and 2.5.1-24). The ancestral Mississippi River appears to have contributed clastics to the Gulf beginning late in the Jurassic – for perhaps 150 million years. An alternative interpretation of regional stratigraphy, structural geology and tectonic is discussed in Subsection 2.5.1.1.4.3.

SSAR subsection 2.5.1.1.4.3 will be revised in a future revision to the ESPA as indicated:

After the relatively rapid phase of continental extension and rifting associated with the opening of the Gulf of Mexico ended, a long period of tectonic quiescence ensued during which the newly passive margin subsided and thick deposits of Late Jurassic and Cretaceous marine sediments accumulated (References 2.5.1-66 and 2.5.1-23). Enormous volumes of sediment were deposited along the northern and northwestern margins of the ancestral Gulf of Mexico by streams draining the interior of North America, causing flexural loading of the crust and progressive southward migration of the shoreline toward the axis of the basin (Reference 2.5.1-33). The long-term migration of the shoreline is marked by bands of offlapping marine strata in the Gulf Coastal Plains that become progressively younger to the south (Figures 2.5.1-2a, 2.5.1-9, and 2.5.1-17). During the period of relative quiescence within the Gulf of Mexico region the early Tertiary Laramide orogeny was occurring along the paleo-west coast of North America. Researchers have suggested that compressional stresses generated by subduction and collision during the orogeny were transmitted to the Gulf of Mexico region and influenced the formation of the San Marcos Arch, Sabine Uplift, and intervening basins (Figure 2.5.1-12) (References 2.5.1-91,and 2.5.1-92). Deformation and thinning of the Cretaceous deposits constrain the timing of this deformation (See description in Subsection 2.5.1.1.4.3.3).

Cox & Van Arsdale (1997, Reference 2.5.1-272) postulate an alternative hypothesis to that proposed by previous investigators for the development of the Mississippi

Embayment. Whereas some investigators have related the Late Cretaceous to early Tertiary subsidence of the Mississippi Embayment to the opening of the Gulf of Mexico, more recent data summarized in the following bullets indicate that the Gulf began to open during the early Jurassic. Reference 2.5.1-272 contends that the formation of the Mississippi Embayment was coeval with the passage of the Mississippi Valley graben system over the Bermuda hotspot at about 90 Ma; based upon the interpretation of several aspects of geologic data:

- Basal deposits of upper Cretaceous gravel flanking the Pascola Arch in the northern embayment are interpreted as indicating reactivation of the arch.
- Subcrops of Jurassic and Early Cretaceous strata define a southwest-plunging arch in the southern embayment.
- Paleocene sediments nonconformably overlie deeply weathered mid-Cretaceous alkalic plutons along the western margin of the embayment.
- Stratigraphic data suggest that Mississippi River sediments began to enter the Gulf of Mexico during the Late Cretaceous.

Cox & Van Arsdale, (2002, Reference 2.5.1-273) provide recently published age dates to further support pre-subsidence uplift of the Mississippi Embayment due to hotspot flux during the Cretaceous superplume mantle event. This alternative hypothesis proposes that the Mississippi River system developed during late Cretaceous subsidence of the Mississippi Embayment and that the Embayment subsided about 60 million years after cessation of sea floor spreading in the Gulf of Mexico.

The VCS site region is located within the northwestern progradational margin of the Gulf of Mexico basin, which extends generally from the eastern edge of the Cordilleran compressional deformation near the border of Mexico and Texas eastward to the western most part of Florida and into the southwestern portion of Alabama (Reference 2.5.1-51). The northwestern progradational margin is subdivided into the interior zone and coastal zone, with the interior zone being the more landward of the two zones (Figure 2.5.1-12). The interior zone is primarily associated with broad, relatively shallow Mesozoic embayments that locally host salt diapir provinces overlying Paleozoic basement. According to Ewing (Reference 2.5.1-51), the principal structures of the interior zone are Mesozoic-age normal faults associated with opening of the Gulf of Mexico. South of the interior zone is the coastal zone, which is characterized by a very thick (6 to 9 miles, or 10 to 15 km) section of Late Mesozoic to Cenozoic strata that buries highly-extended Paleozoic crust and Mesozoic oceanic crust (Reference 2.5.1-51). The boundary between the interior and coastal zones lies along a trend of Lower Cretaceous reefs within the Gulf Coastal Plains section (Figure 2.5.1-12). The location of this reef trend is interpreted as a hinge zone reflecting the transition between thick and thin transitional crust and the greater net subsidence of the thin transitional crust due to sedimentary loading in the basin to the south (References 2.5.1-51 and 2.5.1-47).

New SSAR References

2.5.1-272 Cox, R.T. and Van Arsdale, R.B., *Hotspot origin of the Mississippi embayment and its possible impact on contemporary seismicity*, Engineering Geology, vol. 46, pp. 201-216, 1997.

2.5.1-273 Cox, R.T., and Van Arsdale, R.B. *The Mississippi Embayment, North America: a first order continental structure generated by the Cretaceous superplume mantle event*, Journal of Geodynamics, vol. 34, pp. 163-176, 2002.

RAI 02.05.03-1:

Question:

In SSAR sections 2.5.1 and 2.5.3, you discuss the seismic potential of growth faults in the Gulf Coast region and conclude that the numerous growth faults in the region are gravity-driven, rather than tectonic features, and thus cannot be a source of moderate to large earthquakes. However, the 10 February 2006, Mb 5.5 earthquake, on the continental shelf of the Gulf of Mexico is thought to have occurred on a gravity-driven, shallowly dipping surface at an unknown but probably shallow depth . Dewey and Dellinger (2008) conclude that the dearth of high-frequency energy produced by the earthquake is consistent with either faulting within the sedimentary section or a large landslide. Dokka et al. (2006) attributes the 10 February 2006 and other earthquakes in the immediate vicinity to active tectonic processes, presumably by movement on growth faults within the sedimentary section. The SSAR does not refer to the possibility that the 10 February 2006 earthquake was related to movement on a growth fault in its discussions of the seismic potential of growth faults in the vicinity of the VCS.

In support of 10 CFR 100.23 please provide an examination of the seismic potential of growth faults in the vicinity of the VCS site in the light of the possible relationship between the 10 February 2006 Mb 5.5 earthquake and growth faulting in the Gulf of Mexico.

Dewey, J.W., and Dellinger, J.A., 2008, Location of the Green Canyon (Offshore Southern Louisiana) Seismic Event of February 10, 2006: U.S. Geological Survey Open-File Report 2008-1184, 30 p.

Dokka, R.K., Sella, G.F., and Dixon, T.H., 2006, Tectonic control of subsidence and southward displacement of southeast Louisiana with respect to stable North America: Geophysical Research Letters, v. 33, L23308, doi:10.1029/2006GL027250, 5 p.

Response:

As described in SSAR Section 2.5.1.2.4.2, the general consensus of the scientific community is that growth faults of the Gulf Coastal Plains are aseismic and not capable of generating strong vibratory ground motions. This position is supported by the opinions of numerous experts, large observational datasets, and regulatory positions. As a review of SSAR Section 2.5.1.2.4.2, the following summarizes some of the support for this position:

- A NUREG/CR volume on identifying seismogenic faults (Hanson, Kelson, Angell and Lettis, 1999);
- The USGS classification of growth faults as Class B features for the Quaternary Fault and Fold Database (Wheeler, 1999, 2005);
- The absence of growth faults as a seismic source within the EPRI-SOG and the Lawrence Livermore source models used, per NRC guidance, for probabilistic seismic hazard analyses for nuclear power plants (Bernreuter, Savy, Mensing and Chen, 1989, EPRI, 1986-1989);

- The wide extent of growth faults within the coastal plain (Ewing, 1990, 1991, Ewing and Lopez, 1991) (SSAR Figure 2.5.1-2a and 2.5.1-12) combined with the low seismicity rate for the coastal plain (SSAR Figure 2.5.2-1 and 2.5.2-2), especially around Houston where some of the highest rates of surface deformation associated with growth faults are observed (e.g., Clanton, 1979, Engelkemeir and Khan, 2008, Kreitler, 1976, 1978, Shah and Lanning-Rush, 2005, Sheets, 1979, Verbeek, Ratzlaff and Clanton, 1979); and

- NRC Regulatory Guide 1.208 which describes growth faults as "… not having the capacity to generate damaging vibratory ground motion…" (Section C.2.4 of NRC, 2007).

Despite the evidence against growth faults being capable of generating strong vibratory ground motions, the 10 February 2006 Green Canyon earthquake was evaluated as part of the VCS site ESP with respect to its implication for the seismic potential of growth faults.

The Green Canyon earthquake was felt in coastal Louisiana, Texas and Florida with a maximum intensity of MMI III (NEIC, 2007). The causal mechanism of the earthquake has been studied by Nettles (2007), and she concludes that the seismic data of the event is most consistent with gravity-driven slip on a low-angle detachment (e.g., landslide). This conclusion is based on the lack of high-frequency energy in the waveforms, slow rise time, analysis of focal mechanisms, and the location of the event along the Sigsbee escarpment (i.e., a region where large-scale landslides could occur due to relatively steep slopes of the escarpment compared to more inland areas). Dellinger et al. (2007) support this interpretation of the causal mechanism of the Green Canyon earthquake, but they also state that a conclusive interpretation of the event has yet to be determined. It should be noted that presently no independent research has been conducted to either support or contradict this conclusion, and no other earthquakes within the Gulf of Mexico have been attributed to a landslide mechanism.

The main implication of a "landslide" interpretation of the earthquake with respect to seismic hazard is that large mass movement events along the Sigsbee and similar escarpments may be able to generate small to moderate magnitude earthquakes that are detectable on local and regional seismic networks. The importance of the presence of the escarpment is that the escarpment is the submarine geomorphic feature along which the landslide may have occurred (i.e., there needs to be a space for the landslide to slide into, and there needs to be a lack of confining pressure to resist the landslide). Because there are no Sigsbee-like escarpments within the VCS site vicinity, it is expected that growth faults near the site are not capable of producing an event like the Green Canyon Event. Therefore, this event has no safety significance with respect to the VCS site.

The references cited within the RAI question do not alter this conclusion. Dokka et al. (2006) do not directly discuss the Green Canyon earthquake, and thus they do not directly attribute the earthquake to "active tectonic processes." Instead, Dokka et al. (2006) state that earthquakes onshore and offshore Louisiana "…suggest active tectonic processes." However, Dokka et al. (2006) do not provide any evidence or analysis to support this statement. Dokka et al. (2006) only state that they "suspect" these earthquakes are related to internal deformation in the onshore and offshore region of Louisiana. The authors, again, do not directly discuss the Green Canyon earthquake.

Therefore, there is no new information or data within Dokka et al. (2006) that would suggest revising the consensus opinion outlined above that growth faults do not have the potential to cause significant vibratory ground motions.

The report by Dewey and Dellinger (2008) focuses on the methodology used to determine the location of the Green Canyon earthquake. Dewey and Dellinger (2008) state that, "... the purpose of this report is not to arrive at a definite conclusion or 'preferred speculation' on the cause of the Green Canyon event." However, they go on to say that they are forced to consider the cause of the earthquake in determining the location of the event. Dewey and Dellinger (2008) consider three possible mechanisms of the earthquake: (1) faulting within the crystalline basement, (2) faulting within the sedimentary section, and (3) a landslide within the sedimentary section. Based on the small amount of high-frequency energy released during the earthquake, Dewey and Dellinger (2008) propose a preliminary hypothesis that the event is consistent with either faulting within the sedimentary section or a landslide. Given the preliminary nature of this hypothesis, especially in light of Nettles' work (Nettles, 2007) on the earthquake mechanism and the preponderance of evidence against growth faults being seismically active, there is no new information or data within the paper of Dewey and Dellinger (2008) that would suggest revising the consensus opinion outlined above that growth faults do not have the potential to cause significant vibratory ground motions.

Response References:

Bernreuter, D. L., Savy, J. B., Mensing, R. W. and Chen, J. C., *Seismic Characterization of 69 Nuclear Plant Sites East of the Rocky Mountains: Methodology, Input Data and Comparisons to Previous Results for Ten Test Sites*: Washington, D.C., US Nuclear Regulatory Commission, NUREG/CR-5250, Vol. 1., 81 p, 1989.

Clanton, U., *Faults offsetting land surfaces in southeastern Houston metropolitain area, Texas (Abstract)*: AAPG Bulletin, v. 63, p. 432-432, 1979.

Dellinger, J. A., Dewey, J. W., Blum, J. and Nettles, M., *Relocating and Characterizing the 10 Feb 2006 "Green Canyon" Gulf of Mexico Earthquake Using Oil-Industry Data*: Eos Trans. AGU, v. 88(52), Fall Meet. Suppl., Abstract S13F-01, 2007.

Dewey, J. W. and Dellinger, J. A., *Location of the Green Canyon (Offshore Southern Louisiana) Seismic Event of February 10, 2006*, U.S. Geological Survey, Open File Report 2008-1184, 30 p, 2008.

Dokka, R., Sella, G. F. and Dixon, T. H., *Tectonic control of subsidence and southward displacement of southeast Louisiana with respect to stable North America*: Geophys. Res. Lett., v. 33, p. L23308, 2006.

Engelkemeir, R. M. and Khan, S. D., *Lidar mapping of faults in Houston, Texas, USA*: Geosphere, v. 4, p. 170-182, 2008.

EPRI, *Seismic hazard Methodology for the Central and Eastern United States (NP-4726), Vol. 1-3 & 5-10*, EPRI, 1986-1989.

Ewing, T. E., *The Tectonic Map of Texas*: Austin, TX, University of Texas at Austin, Bureau of Economic Geology, 1990.

Ewing, T. E., *Structural framework*, in Salvador, A., ed., The Geology of North America: the Gulf of Mexico Basin, Volume J: Boulder, CO, Geological Society of America, p. 31-52, 1991.

Ewing, T. E. and Lopez, R. F., *Principal Structural Features Gulf of Mexico Basin*, in Salvador, A., ed., The Gulf of Mexico Basin, Volume J: Boulder, Geological Society of America, p. Plate 2, 1991.

Hanson, K. A., Kelson, K. I., Angell, M. A. and Lettis, W. R., *Techniques for Identifying Faults and Determining Their Origins*: Washington, D.C., US Nuclear Regulatory Commission, NUREG/CR-5503, 461 p, 1999.

Kreitler, C. W., *Fault Control of Subsidence, Houston-Galveston Area, Texas*: Austin, TX, Bureau of Economic Geology, Research Note 5, 17 p, 1976.

Kreitler, C. W., *Faulting and Land Subsidence from Ground-Water and Hydrocarbon Production, Houston-Galveston, Texas*: Austin, TX, Bureau of Economic Geology, Research Note 8, 22 p, 1978.

NEIC, *NEIC Monthly Earthquake Data Report file for event 200602104011*, US Geological Survey, ftp://hazards.cr.usgs.gov/edr/mchedr/, 2007.

Nettles, M., *Analysis of the 10 February 2006: Gulf of Mexico Earthquake from Global and Regional Seismic Data (OTC 19099)*, 2007 Offshore Technology Conference: Houston, TX, p. 1 and 2, 2007.

NRC, *Reg. Guide 1.208: A Performance-Based Approach to Define the Site-Specific Earthquake Ground Motion*, US NRC, 53 p, 2007.

Shah, S. D. and Lanning-Rush, J., *Principal faults in the Houston, Texas metropolitan area*, U.S. Geological Survey, Scientific Investigations Map 2874, 2005.

Sheets, M. M., *Oil Fields, Subsidence and Surface Faulting in the Houston Area*: Houston, TX, Houston Geological Society, Guidebook for 1979 AAPG/SEPM Convention in Houston, TX, 23 p, 1979.

Verbeek, E. R., Ratzlaff, K. W. and Clanton, U. S., *Faults in Parts of North-Central and Western Houston Metropolitan Area, Texas*: Reston, VA, US Geological Survey, Miscellaneous Field Studies Map 1136, 1979.

Wheeler, R. L., *Fault number 924, Gulf-margin normal faults, Texas, in Quaternary fault and fold database of the United States*, USGS, http://earthqakes.usgs.gov/regional/qfaults, 1999.

Wheeler, R. L., *Known or Suggested Quaternary Tectonic Faulting, Central and Eastern United States—New and Updated Assessments for 2005*, U.S. Geological Survey Open-File Report 2005-1336, 40 p, 2005.

Associated ESPA Revision:

No ESPA revision is required as a result of this response.

ATTACHMENT 7

SUMMARY OF REGULATORY COMMITMENTS

(Exelon Letter to USNRC, NP-11-0024, dated June 16, 2011)

The following table identifies commitments made in this document. (Any other actions discussed in the submittal represent intended or planned actions. They are described to the NRC for the NRC's information and are not regulatory commitments.)

COMMITMENT	COMMITTED DATE	COMMITMENT TYPE	
		ONE-TIME ACTION (Yes/No)	Programmatic (Yes/No)
Exelon will revise the VCS ESPA SSAR Section 2.5.1 to incorporate the change shown in the enclosed response to the following NRC RAI: 02.05.01-19 (Attachment 5)	Revision 1 of the ESPA SSAR and ER planned for no later than March 31, 2012	Yes	No